## Materials Today: Proceedings

# An Integrated Computer Vision System for Real-time Monitoring and Control of Long-fiber Embedded Hydrogel 3D Printing

Wenhuan Sun<sup>a</sup>, Victoria Webster-Wood<sup>a,b,</sup>1

<sup>a</sup>Department of Mechanical Engineering, 5000 Forbes Ave, Pittsburgh, 15213, United States <sup>b</sup>Department of Biomedical Engineering, 5000 Forbes Ave, Pittsburgh, 15213, United States

#### **Abstract**

3D printed hydrogel components have been used in a wide range of applications including tissue engineering and soft and biohybrid robotics. Advances in embedded printing, such as the Freeform Reversible Embedding of Suspended Hydrogels (FRESH), have further improved the geometric fidelity of 3D printed hydrogels using a fugitive support bath. Recently, it has been shown that the structural rigidity of hydrogels fabricated with embedded 3D printing can be significantly reinforced for a wider range of applications using the Long-fiber Embedded FRESH (LFE-FRESH) technique, an extension of FRESH by combing fiber embedding and hydrogel 3D printing. However, fibers are prone to buckling under compression load due to the high slenderness ratio and maintaining fiber stability during embedding is vital for LFE-FRESH. In this study, we introduce an integrated computer vision (CV) system for the continuous monitoring and control of LFE-FRESH, which actively adjusts the fiber embedding process in real-time by quantifying fiber deformation from the video data and controlling the fiber extrusion motor. Using the prototype, we demonstrated that the integrated CV system effectively prevents fiber buckling, corrects for over-extrusion during the LFE-FRESH process, and improves fiber embedding quality. Moreover, this technique was implemented with low-cost, mass-produced components and can be conveniently integrated with existing open-source LFE-FRESH software and hardware, which improves its accessibility and facilitates future adaptations for new research applications.

Keywords: fiber embedding; computer vision; multi-material printing; hydrogel; LFE-FRESH; FRESH printing

## 1. Introduction

Natural and synthetic hydrogels are porous and hydrophilic polymer networks with a wide range of attractive properties when compared to other engineering materials, such as biocompatibility and variable material properties based on chemical composition and fabrication methods. Moreover, some hydrogels can respond to changing environmental cues and thus be used as stimuli-response smart materials, such as hydrogels with humidity and temperature-dependent swelling ratios [1]. Due to these unique properties, hydrogels have been widely used in numerous applications, including soft and biohybrid robotics[2], tissue engineering[3], drug delivery[4], and microfluidics[5].

Traditional hydrogel assembly methods, such as electrospinning and die-casting, have limited 3D geometry forming capability. In comparison, hydrogel 3D printing has emerged as a versatile and powerful tool with greatly expanded geometric design freedom. However, 3D printing complex structures using hydrogels without simultaneously printing proper support material remains challenging because many hydrogels are not strong enough to support their own weight during printing. To overcome this, a wide range of embedded printing methods have been introduced, which avoid support structure printing by directly assembling hydrogels in a granular, gel-based, fugitive support bath. Such support bath material traps the hydrogel in place during printing and crosslinking and liquefies post-printing for part retrieval [6–15]. For example, Freeform Reversible Embedding of Suspended Hydrogels (FRESH) is a state-of-theart embedded printing technique that uses a support bath made of gelatin micro-particles [16]. To date, FRESH has been used to successfully print hydrogels structures with a wide range of 3D geometry, functions, sizes, and bio-ink materials with a great spatial resolution (~ 20 µm) [16–19].

E-mail address: vwebster@andrew.cmu.edu

<sup>\*</sup> Corresponding author. Tel.: +1-412-268-3017.

Despite the impressive shape forming capability, FRESH printed hydrogels typically exhibit weak mechanical strength, which limits their applications, especially those that require higher load-bearing capacity. To tackle this, an extension to FRESH has been introduced, termed Long-fiber Embedded FRESH (LFE-FRESH). LFE-FRESH combines long-fiber embedding with hydrogel 3D printing and has been demonstrated to significantly improve the tensile modulus and strength of FRESH printed hydrogels [20].

Although LFE-FRESH has enabled significant structural reinforcement of 3D printed hydrogels, fibers are prone to buckling during the embedding process due to the compression load on the fiber and its high slenderness ratio. Fiber buckling can cause print failure and result in loss of valuable bio-ink and fiber materials [20]. While a theoretical lower bound on the fiber tensile modulus given bio-ink properties was previously developed to assist users of LFE-FRESH to select suitable fiber-bio-ink combinations, the underlying modeling of the lower bound is based on the assumption that fibers have isotropic material properties with a circular cross-sectional area. However, in many applications, such assumptions do not hold due to the unique properties of the fiber material. For example, electrochemically aligned collagen (ELAC) fibers used in the LFE-FRESH process have anisotropic material distribution and non-circular cross-sectional geometries [21]. In this case, the fiber may buckle unexpectedly and lead to catastrophic print failure. To prevent fiber buckling and subsequent print failure and material loss, methods to monitor and adjust the fiber embedding process in real-time are needed. Due to the small size of the fiber extruder mechanism used in LFE-FRESH, manually monitoring the process by eye is labor-intensive and extremely difficult. In addition, in the event of fiber buckling, one may not have enough time to send correction or termination G-code to adjust the fiber embedding process and many 3D printers do not support such in-print extrusion adjustment features.

Here, we report the development of an integrated computer vision (CV) system to enable the continuous monitoring and control of the LFE-FRESH process, which actively adjusts the fiber embedding process in real-time by quantifying transverse (perpendicular to the fiber's axis) fiber deformation from video data. To achieve this, we designed a CV platform consisting of a commercially available USB microscope, 3D printed support plate, mass-produced standard hardware, and off-the-shelf electronics, which can be adjusted to capture different levels of details of the fiber extruding mechanism. After introducing the mechanical and electrical system design, we present the algorithm design that enables the decision-making process of the CV system and showcase its fiber buckling prevention performance with two types of fiber: single-ply polyester and ELAC fibers. Finally, we demonstrate the system's capabilities in correcting fiber over-extrusion and improving fiber embedding fidelity. With low build cost and easy integration with the existing LFE-FRESH software and hardware, the presented CV system is a valuable addition to the LFE-FRESH platform as it improves the usability and robustness of long-fiber embedded hydrogel 3D printing for existing and new research applications.

#### 2. Materials and methods

## 2.1. Mechanical design

The mechanical fixture design of the CV system provides adjustable, stable support for the camera. The CV system uses a low-cost USB microscope (1000x, Jiusion), which is gripped in place by a 3D printed camera retaining ring (Fig. 1A). This design allows for one degree of freedom (rotation about the long axis of the camera body) when other components are fixed, which facilitates manual adjustment of camera angle after installation so that the fiber aligns with the longer edge of the frame. The camera retaining ring is bonded with a 3D printed core plate, which moves along three threaded rods (M3 x 120 mm, McMaster-Carr). Once moved to the desired location, the linear translation of the core plate can be constrained by a set of distance adjust fasteners (M3 x 12mm x 4mm Lock Adjusting Nut, Uxcell). The threaded rods are secured onto the stepper motor of the fiber extruder with three locknuts. The microscope magnification can be tuned by turning the magnification adjustment knob to capture different levels of detail within the fiber extruding mechanism. When the magnification is adjusted, the distance between the camera and the fiber extruder should be adjusted accordingly to accommodate the changing focal length (Fig. 1B).

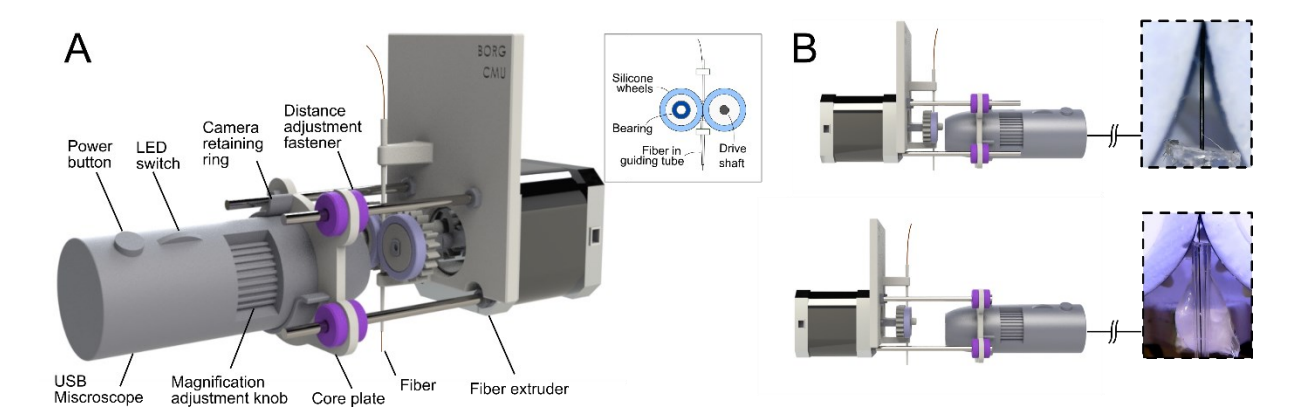


Fig. 1. Real-time monitoring and control of long-fiber embedded hydrogel 3D printing (LFE-FRESH) are performed using an integrated computer vision system (A) Schematic drawing of the computer vision system mounted onto a fiber extruder. Inset shows key components of the fiber extruder; (B) Imaging magnification can be adjusted to capture different levels of details of the fiber embedding mechanism, such as high magnification mode that focus on the unconstrained fiber section (upper) and low magnification mode that covers the entire fiber guiding tube (lower).

## 2.2. The CV Assisted LFE-FRESH process

The LFE-FRESH process is a multi-material additive manufacturing method, which was recently developed by our group to improve the structural rigidity of FRESH printed hydrogels [20]. The CV-assisted LFE-FRESH follows the original LEF-FRESH process with slight modification. Briefly, before printing, compacted gelatin support bath material is transferred to a printing container and hydrogel bio-ink is loaded in a Replistruder syringe pump [22] (Fig. 2). At room temperature, the needle is positioned at the desired start point and the FRESH printing of a hydrogel structure is started with Replicator G (http://replicat.org/). Subsequently, a section of fiber is loaded into the fiber extruder and positioned at the start point. The CV system is switched on before fiber embedding is executed using ReplicatorG. The CV system continuously monitors the fiber embedding process and adjusts fiber extrusion motion to prevent fiber buckling. Finally, the embedded fiber is cut from the fiber extruder and the printing container is incubated at 37 °C for 15 min for support liquefaction and part retrieval. Readers interested in a detailed description of the material preparation (ELAC fiber, FRESH slurry, hydrogel bio-ink) and printing process are encouraged to refer to the original LFE-FRESH and ELAC fabrication papers [20,21,23].

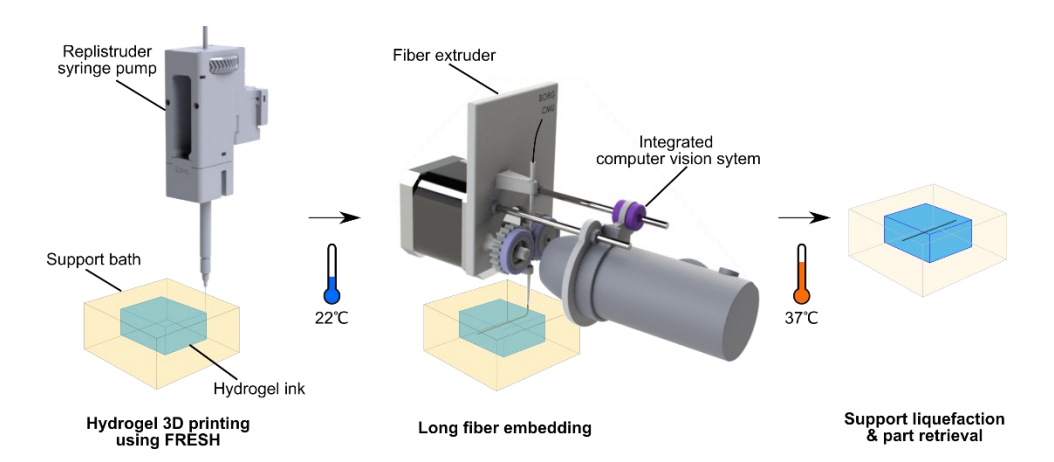


Fig. 2. Schematic drawing of the long-fiber embedded hydrogel 3D printing process. A layer of hydrogel is 3D printed into the support bath using the Free-form Reversible Embedding of Suspended Hydrogel (FRESH) technique (left), and a long-fiber is embedded in the hydrogel (middle). Support bath material liquefies upon raised temperature (37 °C), enabling part retrieval (right).

#### 2.3. Electrical and control system design

During LFE-FRESH, the fiber embedding process is executed via the serial communication between a computer and a 3D printer (Fig. 3) following a predefined G-code. In parallel, the computer receives video data from the CV system and makes extrusion adjustment decisions in real-time based on captured fiber deflection using the developed control algorithm (Fig. 4). When observing excess fiber deflection, the computer sends a command to a microcontroller (UNO, ELEGOO) via serial communication, which temporarily deactivates the fiber extruder motor via a relay module (5V-4-Channel, JBtek Electric Solutions) until the excess fiber deformation is resolved. However, such motor deactivation may cause the 3D printer control board to reset its serial communication with the computer, leading to unexpected print termination. To address this, a standby motor is connected to the 3D printer's motor driver. During normal embedding, the standby motor shares the same signal and works in parallel with the fiber extruder motor.

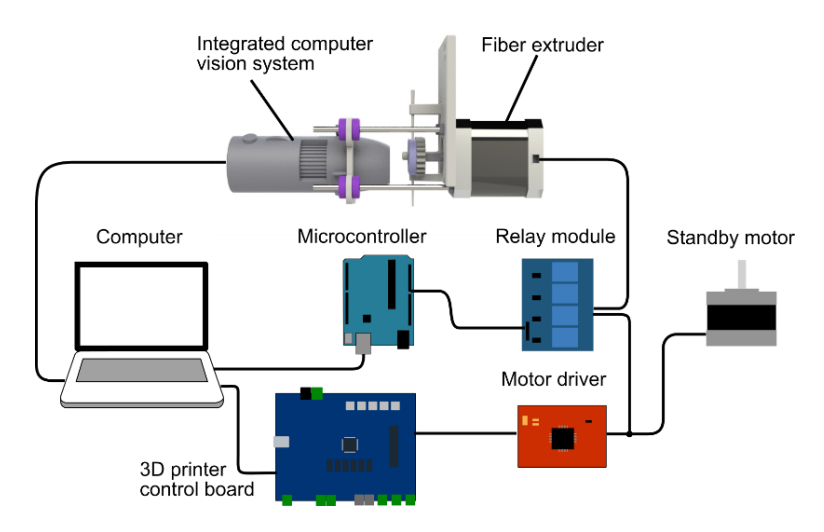


Fig. 3. Schematic drawing of the integrated computer vision monitoring and control hardware system. The computer sends G-code to the 3D printer control board to perform hydrogel 3D printing and long-fiber embedding. During printing, it receives and processes video data from the computer vision system, determines fiber status, and sends commands to the microcontroller, which adjusts the actuation of the fiber extruder in real-time to prevent fiber buckling. A standby motor is connected to the motor driver to avoid unexpected serial connection reset due to fiber extruder motor deactivation.

The CV control algorithm running on the computer quantifies the fiber's transverse (perpendicular to the length of the fiber) deflection and sends adjustment commands to the microcontroller as needed (Fig. 4). Briefly, the computer first receives a frame from the CV system, which is converted to an 8-bit grayscale format. Based on the difference in pixel intensity between the fiber (dark) and the extruding mechanism (light), a pixel intensity threshold is applied to locate the mass of fiber pixels for subsequent steps. After that, a frame masking filter is applied to isolate fiber pixels and the sample standard deviation of the transverse coordinate of fiber pixels is calculated and compared against a predefined threshold. If the variance exceeds the threshold, the computer sends a command to the microcontroller to temporarily pause fiber feeding before entering the next iteration. The average processing time for the algorithm is 30 ms, the camera operates at a frame rate of 30 fps (frame-per-second), and the relay module has a response time of 10 ms. Overall, the maximum control frequency of the CV system is 13.5 Hz. The algorithm is designed to tolerate translation of the fiber within the frame as long as the initial fiber orientation aligns with the long axis of the frame. Additionally, the fiber pixel distribution threshold is adjusted before printing to ensure appropriate sensitivity, which captures excess fiber deflection due to buckling while tolerating minor deflection due to vibration. Specifically, the threshold in this work was set to be 2.2 times the sample standard deviation of pixel coordinates measured before fiber embedding.

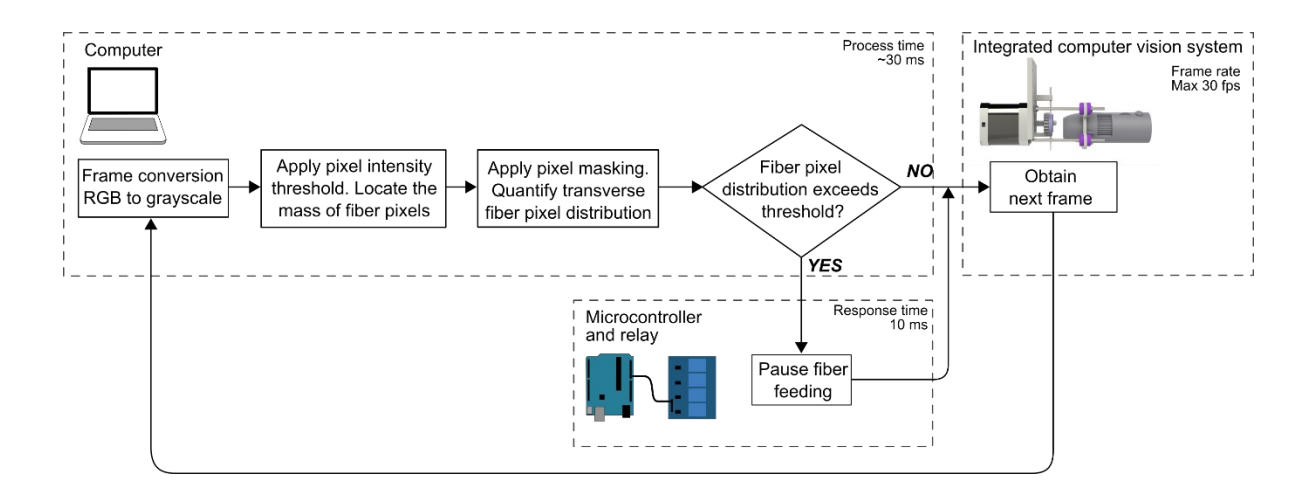


Fig. 4. Computer vision control algorithm flow chart. In each iteration, the computer receives one frame from the video data captured by the computer vision system. Color conversion, pixel intensity thresholding, and pixel masking procedures are subsequently applied to the frame to obtain the transverse fiber pixel distribution. If the sample variance of such distribution exceeds a pre-defined threshold, the computer sends a command to the microcontroller module to pause fiber feeding.

## 3. Results and discussion

## 3.1. Integrated CV system prevents material loss due to fiber buckling

The control algorithm of the CV-assisted LFE-FRESH process is based on the detection of excess transverse fiber deflection as an indicator of fiber buckling when compared against a predefined threshold. To demonstrate its differentiation capability of the CV system, the CV system was first tested using a single-ply polyester sewing thread, which has a uniform cross-sectional shape, surface texture, and color (Fig. 5A, B). During normal embedding, the fiber remains straight with slight rotation, which leads to a highly concentrated distribution of transverse fiber pixels around the sample mean (Fig. 5A). In comparison, during fiber buckling, the bending of the fiber leads to dispersion of transverse fiber pixels with significantly higher sample variance (p-value < 0.01) (Fig. 5B). Similarly, when using ELAC fiber, a material with less uniform surface texture and color, fiber buckling leads to a significantly higher variance (p-value < 0.01) (Fig. 5C, D). Based on the significant difference of the fiber deflection amount between normal and buckled fibers, the CV system effectively terminates fiber embedding process in the event of fiber buckling to prevent further loss of materials.

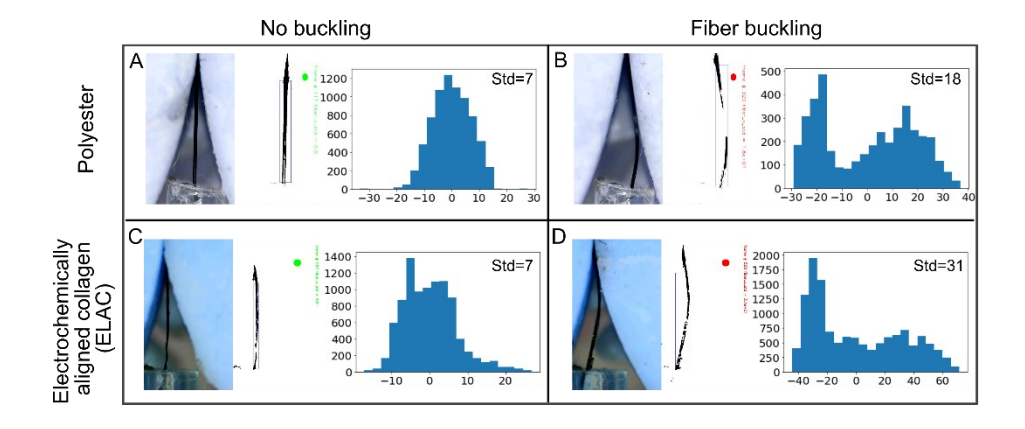


Fig. 5. The integrated computer vision system prevents material loss due to embedding failure by identifying fiber buckling using transverse fiber pixel distribution. Two fiber conditions (buckling and no buckling) of two fiber types (polyester and electrochemically aligned collagen (ELAC)) are demonstrated. In each cell, a representative frame image from the camera (left), identified fiber pixels (middle), and histogram and sample standard deviation of transverse pixel distribution (right) are displayed. The x-axis of the histogram is unitless values of transverse fiber pixels.

## 3.2. Integrated CV system corrects over-extrusion and improves fiber embedding quality

Similar to its counterpart in Fused Deposition Modeling (FDM) 3D printing [24,25], over-extrusion during fiber embedding occurs when the fiber extrudes an excess amount of fiber material out of the fiber guiding tube. In addition to the defects introduced by over-extrusion in traditional FDM 3D printing, such as dimensional inaccuracy and surface defects, over-extrusion during fiber embedding can also cause catastrophic print failure, including fiber buckling and subsequent fiber clogging, where the fiber escapes from the unconstrained section and causes print failure (Fig. 6A). To demonstrate the over-extrusion correction capability of the CV system, an input geometry of an S-shaped fiber embedding pattern within an alginate bio-ink block was implemented (Fig. 6A). For all experiments, an overextrusion of 20% was added to the fiber embedding process and two types of ELAC fibers were tested. When using the flexible ELAC fiber that is prone to fiber buckling upon over-extrusion, the CV system was able to correct for over-extrusion and the difference between the embedded fiber length and the input geometry is not statistically significant (Fig. 6C, upper left, input fiber length without over-extrusion: 30.566 mm, embedded fiber length: 29.5 mm, p-value = 0.31). In comparison, when the CV system was not activated, fiber-buckling causes fiber embedding failure, and a partially embedded fiber section was dragged and moved with the fiber guiding tube (Fig. 6C, lower left). Compared with flexible fibers, stiff fibers are not prone to buckling upon over-extrusion without CV correction. Instead, they overcome the constraint of the host hydrogels and often bend or deflect into unpredictable shapes within the hydrogel (Fig. 6C, lower right). When the CV system is activated when printing stiff fibers with over-extrusion, the fiber embedding quality was improved (Fig. 6C, upper right), because the fiber undergoes frequent side-way movements even though it does not buckle, which the algorithm detected and adjusted for.

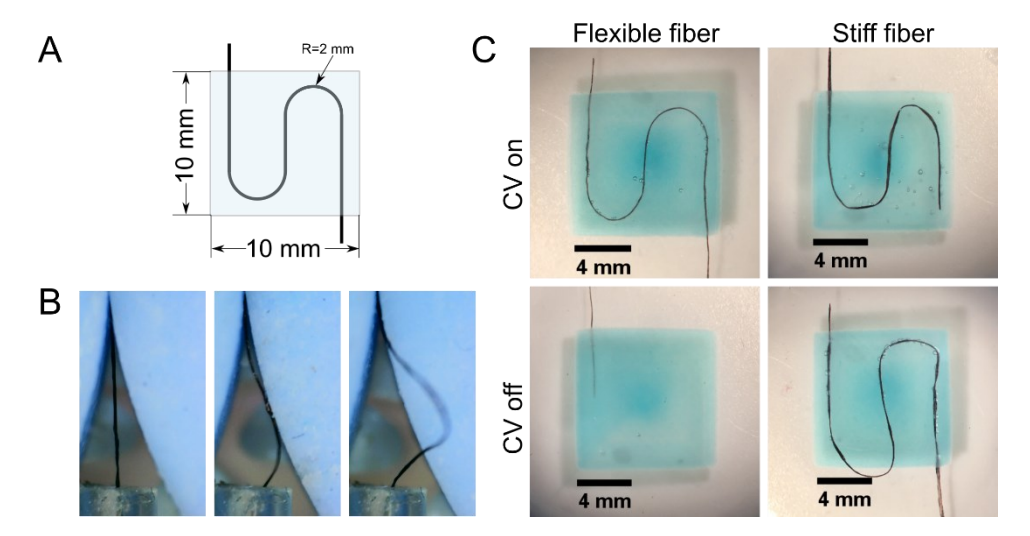


Fig. 6. CV-assisted LFE-FRESH corrects over-extrusion and improves fiber embedding quality. (A). Input geometry of the hydrogel structure (gray) and fiber print path (black) (B). Time series frame image of a fiber buckling, and clogging process caused by over-extrusion. (C). A grid view of the embedding results comparison using two software settings (CV system turned on and off) and two fiber materials (stiff and flexible).

### 4. Conclusion

In this work, we introduced a computer vision-assisted LFE-FRESH printing process as an extension to the existing LFE-FRESH method for real-time monitoring and process control. The LFE-FRESH process has been previously

demonstrated to enable significant structural reinforcement of 3D printed hydrogel components [20]. In this study, we addressed one major constraint of LFE-FRESH, fiber buckling, which can be induced by insufficient fiber mechanical properties, fiber defects, and over-extrusion and can cause print failure and material loss. The integrated CV system monitors and adjusts the fiber feeding motion by quantifying the transverse fiber deflection. In addition to fiber-buckling prevention, the CV system can also correct for over-extrusion and improve fiber embedding quality. In the future, the robustness of the CV system can be further improved by incorporating a machine learning trained fiber buckling predictor that accommodates variation in fiber orientation. In addition, the USB serial communication used in this study can be replaced with wireless options, such as a microscope with a Wi-Fi module, to further reduce vibration during printing. With low material cost and easy integration with the existing open-source LFE-FRESH software and hardware, the presented CV system is a valuable extension to the LFE-FRESH method that improves the usability and robustness of long-fiber embedded hydrogel 3D printing for existing and new research applications.

## Acknowledgements

This work was supported by an NSF CAREER award under Grant No. ECCS-2044785, the William and Barbara Goldsmith Family Fellowship, the Presidential Fellowship in the College of Engineering at Carnegie Mellon University, and a Carnegie Mellon University (CMU) Department of Mechanical Engineering Collaborative Fellowship.

## References

- [1] W. Sun, S. Schaffer, K. Dai, L. Yao, A. Feinberg, V. Webster-Wood, 3D Printing Hydrogel-Based Soft and Biohybrid Actuators: A Mini-Review on Fabrication Techniques, Applications, and Challenges, Front. Robot. AI. 8 (2021) 1–10. https://doi.org/10.3389/frobt.2021.673533.
- [2] V.A. Webster-Wood, O. Akkus, U.A. Gurkan, H.J. Chiel, R.D. Quinn, Organismal engineering: Toward a robotic taxonomic key for devices using organic materials, Sci. Robot. 2 (2017) eaap9281. https://doi.org/10.1126/scirobotics.aap9281.
- [3] T. Billiet, M. Vandenhaute, J. Schelfhout, S. Van Vlierberghe, P. Dubruel, A review of trends and limitations in hydrogel-rapid prototyping for tissue engineering, Biomaterials. 33 (2012) 6020–6041. https://doi.org/10.1016/j.biomaterials.2012.04.050.
- [4] J. Li, D.J. Mooney, Designing hydrogels for controlled drug delivery, Nat. Rev. Mater. 1 (2016). https://doi.org/10.1038/natrevmats.2016.71.
- [5] U.N. Lee, J.H. Day, A.J. Haack, R.C. Bretherton, W. Lu, C.A. Deforest, A.B. Theberge, E. Berthier, Layer-by-layer fabrication of 3D hydrogel structures using open microfluidics, Lab Chip. 20 (2020) 525–536. https://doi.org/10.1039/c9lc00621d.
- [6] K.J. Leblanc, S.R. Niemi, A.I. Bennett, K.L. Harris, K.D. Schulze, W.G. Sawyer, C. Taylor, T.E. Angelini, Stability of High Speed 3D Printing in Liquid-Like Solids, ACS Biomater. Sci. Eng. 2 (2016) 1796–1799. https://doi.org/10.1021/acsbiomaterials.6b00184.
- [7] J. Zhao, M. Hussain, M. Wang, Z. Li, N. He, Embedded 3D printing of multi-internal surfaces of hydrogels, Addit. Manuf. 32 (2020) 101097. https://doi.org/10.1016/j.addma.2020.101097.
- [8] T.G. Molley, G.K. Jalandhra, S.R. Nemec, A.S. Tiffany, A. Patkunarajah, K. Poole, B.A.C. Harley, T.T. Hung, K.A. Kilian, Heterotypic tumor models through freeform printing into photostabilized granular microgels, Biomater. Sci. 9 (2021) 4496–4509. https://doi.org/10.1039/d1bm00574j.
- [9] Y. Jin, A. Compaan, T. Bhattacharjee, Y. Huang, Granular gel support-enabled extrusion of three-dimensional alginate and cellular structures, Biofabrication. 8 (2016). https://doi.org/10.1088/1758-5090/8/2/025016.
- [10] Y. Zhang, S.T. Ellison, S. Duraivel, C.D. Morley, C.R. Taylor, T.E. Angelini, 3D printed collagen structures at low concentrations supported by jammed microgels, Bioprinting. 21 (2021) e00121. https://doi.org/10.1016/j.bprint.2020.e00121.
- [11] T. Bhattacharjee, C.J. Gil, S.L. Marshall, J.M. Urueña, C.S. O'Bryan, M. Carstens, B. Keselowsky, G.D. Palmer, S. Ghivizzani, C.P. Gibbs, W.G. Sawyer, T.E. Angelini, Liquid-like Solids Support Cells in 3D, ACS Biomater. Sci. Eng. 2 (2016) 1787–1795. https://doi.org/10.1021/acsbiomaterials.6b00218.

- [12] K. Hajash, B. Sparrman, C. Guberan, J. Laucks, S. Tibbits, Large-scale rapid liquid printing, 3D Print. Addit. Manuf. 4 (2017) 123–131. https://doi.org/10.1089/3dp.2017.0037.
- [13] S.R. Moxon, M.E. Cooke, S.C. Cox, M. Snow, L. Jeys, S.W. Jones, A.M. Smith, L.M. Grover, Suspended Manufacture of Biological Structures, Adv. Mater. 29 (2017). https://doi.org/10.1002/adma.201605594.
- [14] A.M. Compaan, K. Song, Y. Huang, Gellan Fluid Gel as a Versatile Support Bath Material for Fluid Extrusion Bioprinting, ACS Appl. Mater. Interfaces. (2019). https://doi.org/10.1021/acsami.8b13792.
- [15] O. Jeon, Y. Bin Lee, H. Jeong, S.J. Lee, D. Wells, E. Alsberg, Individual cell-only bioink and photocurable supporting medium for 3D printing and generation of engineered tissues with complex geometries, Mater. Horizons. 6 (2019) 1625–1631. https://doi.org/10.1039/c9mh00375d.
- [16] T.J. Hinton, Q. Jallerat, R.N. Palchesko, J.H. Park, M.S. Grodzicki, H.-J. Shue, M.H. Ramadan, A.R. Hudson, A.W. Feinberg, Three-dimensional printing of complex biological structures by freeform reversible embedding of suspended hydrogels, Sci. Adv. 1 (2015) 1–10. https://doi.org/10.1126/sciadv.1500758.
- [17] A. Lee, A.R. Hudson, D.J. Shiwarski, J.W. Tashman, T.J. Hinton, S. Yerneni, J.M. Bliley, P.G. Campbell, A.W. Feinberg, 3D bioprinting of collagen to rebuild components of the human heart, Science (80-.). 365 (2019) 482–487. https://doi.org/10.1126/science.aav9051.
- [18] E. Mirdamadi, J.W. Tashman, D.J. Shiwarski, R.N. Palchesko, A.W. Feinberg, FRESH 3D bioprinting a full-size model of the human heart, ACS Biomater. Sci. Eng. (2020) 0–6. https://doi.org/10.1021/acsbiomaterials.0c01133.
- [19] T.J. Hinton, A. Lee, A.W. Feinberg, 3D bioprinting from the micrometer to millimeter length scales: Size does matter, Curr. Opin. Biomed. Eng. 1 (2017) 31–37. https://doi.org/10.1016/j.cobme.2017.02.004.
- [20] W. Sun, J.W. Tashman, D.J. Shiwarski, A.W. Feinberg, V.A. Webster-wood, Long-Fiber Embedded Hydrogel 3D Printing for Structural Reinforcement, ACS Biomater. Sci. Eng. (2021). https://doi.org/10.1021/acsbiomaterials.1c00908.
- [21] W. Sun, J. Paulovich, V. Webster-Wood, Tuning the Mechanical and Geometric Properties of Electrochemically Aligned Collagen Threads Toward Applications in Biohybrid Robotics, J. Biomech. Eng. 143 (2021). https://doi.org/10.1115/1.4049956.
- [22] J.W. Tashman, D.J. Shiwarski, A.W. Feinberg, A high performance open-source syringe extruder optimized for extrusion and retraction during FRESH 3D bioprinting, HardwareX. 9 (2021) e00170. https://doi.org/10.1016/j.ohx.2020.e00170.
- [23] X. Cheng, U.A. Gurkan, C.J. Dehen, M.P. Tate, H.W. Hillhouse, G.J. Simpson, O. Akkus, An electrochemical fabrication process for the assembly of anisotropically oriented collagen bundles, Biomaterials. 29 (2008) 3278–3288. https://doi.org/10.1016/j.biomaterials.2008.04.028.
- [24] Z. Jin, Z. Zhang, G.X. Gu, Autonomous in-situ correction of fused deposition modeling printers using computer vision and deep learning, Manuf. Lett. 22 (2019) 11–15. https://doi.org/10.1016/j.mfglet.2019.09.005.
- [25] R. Comminal, M.P. Serdeczny, D.B. Pedersen, J. Spangenberg, Motion planning and numerical simulation of material deposition at corners in extrusion additive manufacturing, Addit. Manuf. 29 (2019) 100753. https://doi.org/10.1016/j.addma.2019.06.005.